Alexandria Engineering Journal (2016) 55, 2431–2438

HOSTED BY

ELSEVIER

Alexandria University

Alexandria Engineering Journal

www.elsevier.com/locate/aej
www.sciencedirect.com

ORIGINAL ARTICLE

Grain refinement of ASTM A356 aluminum alloy using sloping plate process through gravity die casting

Adnan Mehmood [a], **Masood Shah** [a], **Nadeem Ahmed Sheikh** [b,*], **Junaid Ahmad Qayyum** [a], **Shahab Khushnood** [a]

[a] *Department of Mechanical Engineering, Faculty of Mechanical & Aeronautical Engineering, University of Engineering and Technology, Taxila, Pakistan*
[b] *Department of Mechanical Engineering, Capital University of Science and Technology, Islamabad, Pakistan*

Received 26 July 2015; revised 14 March 2016; accepted 15 March 2016
Available online 10 May 2016

KEYWORDS

Grain refinement;
Sloping plate;
Nucleation;
Thermal boundary layer;
Viscous boundary layer

Abstract Sloping plate flow is used for enhancement of material properties through grain refinement in gravity die casting of Aluminum alloy ASTM A356. The castings are prepared with different slope angles of an 800 mm long, naturally cooled stainless steel plate. The specimens obtained are then tested for tensile strength and elongation. Microstructure of the cast specimens is observed and conclusions drawn on the grain size and precipitate morphology as a function of angle of sloping plate. Analysis is presented for the boundary layer created while the material flows over the plate. An indication of the boundary layer thickness is determined by measuring the thickness of the residual metal layer on the plate after casting. An analytical solution of the boundary layer thickness is also presented. It is shown that the calculated boundary layer thickness and the thickness of the layer of material left in the channel after casting are in good agreement. Moreover, microstructure examination and tensile tests show that best properties are achieved with a 60° sloping plate.

1. Introduction

Producing near net shape in a metallic material in semisolid form is termed as "semi-solid processing" [1]. Since 1990s Semi-Solid Metallurgy (SSM) is focused on aluminum and its alloys and today many of the parts made by this technique are replacing the conventionally processed (Sand casting, Gravity casting, etc.) parts. SSM processing has been subjected to extensive research, development and commercialization attempts after the year 2000 [2,3]. The overall field of SSM comprises today a large number of specific process routes, almost all of which fall in the category of either "Rheocasting" or Thixocasting." The former begins with liquid metal and involves agitation during partial solidification followed by forming. The latter begins with solid metal of suitable structure

* Corresponding author.

Peer review under responsibility of Faculty of Engineering, Alexandria University.

http://dx.doi.org/10.1016/j.aej.2016.03.016

and involves heating to the desired solid fraction and forming [4].

Grain refinement is achieved by controlling the size of grain structure formed during solidification process by different techniques [5]. Grain refinement can be performed by using mechanical (introducing ultrasonic vibration during nuclei formation), chemical (inoculant addition) and thermal (time and Temperature and control) techniques [6–11].

Amount of heat extraction into a melt, rate of nucleation, and temperature on which molten poured are the influencing factors for specimen, manufactured by semi-solid forming methods [12]. By avoiding the cast defects such as micro- and macro-shrinkage cold shuts design manufacturability can be achieved [13]. Cooling plate process is used to transform microstructure from dendritic to globular shape by detachment of nuclei or shearing effect. The sloping plate processing is a useful technique for preparing slurry due to its low cost and high efficiency. A low superheated melt is poured on slope to form slurry [14]. High rate of cooling (up to 1000 K/s for certain metals) and process temperature control results in the refinement of microstructure. Flow velocities over cooling plate affect the cooling rate and result in meta-rapid solidification at low flow velocities and folding effect at high flow velocities. Stirring action produced globular grain instead of dendritic metal in a semi-solid state and its viscosity is also low [1,15,16]. Mathematical modeling shows solid fraction produced during casting process is the same as compared with experimental [17].

Sloping channel can be made by different materials such as mild steel [18,19] aluminum and copper [20,21] and many of other materials and different types of cooling media such as water and oil can be used. Flow behavior of the ASTM A356 Alloy on sloping plate is predicted [22] with the help of flow Reynolds number, where the two flow regimes either streamline or turbulent are dependent on angle of plate. Guan in 2007 published his work on sloping plate for Al3%Mg Semisolid alloy preparation, in which 3D simulation model was developed in ANSYS and simulation showed that angle of plate will greatly affect the velocity of molten metal and as result temperature will also be effected. Temperature and velocity increase at the end as the slop angle increases [23].

Introducing wave slope is good for producing finer spherical like grain with short globular structure and burst nucleation to produce more nucleation sites which result in structure improvement [24]. Two types of nucleation, heterogeneous and homogenous, play major role, as heterogeneous nucleation increases, the size of grains formed decreases [25]. The preparation of slurry plays an important role in terms of good microstructure and properties. Mechanical stirring [26], magneto hydro dynamic (MHD) stirring [27], melt conditioner direct chill casting [28], bubble stirring and so on processes are the most practicing slurry preparation processes used today.

This research is based on the analysis of the effect of the sloping plate on the mechanical properties and microstructure. The stirring caused by the sloping plate is related to the boundary layer produced on the sloping plate. The analysis of the boundary layer is compared with the actual residual metal left in the sloping plate after flow. This is then compared with a model developed specifically for this purpose. The results of analytical modeling of boundary layer thickness are compared with the experimentation techniques and the different mechanical properties are compared with the angle of the flowing sloping plate.

2. Analysis of flow of molten metal on sloping plate

The extent of the boundary layer and nucleation depends on the heat transfer coefficient, Reynold's number, flow velocity and temperature of molten material. The steady state heat convection of molten metal flow over a flat surface can be modeled as,

$$U\frac{\partial T}{\partial x} = \alpha\frac{\partial^2 T}{\partial y^2} \tag{1}$$

where U is the mean flow velocity along the plate (x-direction), T is the temperature of the fluid with y-direction perpendicular to the surface and α is the thermal diffusivity. The hot molten metal experiences temperature gradient at the wall due to difference in the temperatures leading to the formation of thermal boundary layer, δ_T. Using Eq. (1) and in light of above discussion a formulation for the thermal boundary layer can be deduced as [29],

$$\delta_T = 3.6\sqrt{\frac{\alpha x}{U}} \tag{2}$$

With the change in the slope angle, θ, of the flat plate, the mean flow velocity can be modeled using [29],

$$U = \frac{\gamma sin\theta}{\mu}\left(yd + \frac{1}{2}y^2\right) \tag{3}$$

where γ is the Specific weight of the flowing molten metal and d is the width of the channel. For the flowing steady stream of fluid, formation of viscous boundary layer, δ_u, due to the viscous forces can be estimated as [29],

$$\delta_u = 5.0\sqrt{\frac{vx}{U}} \tag{4}$$

In liquid molten metals both thermal and viscous boundary layers can be related as [30],

$$\frac{\delta_u}{\delta_T} = 0.72Pr^{1/2} \tag{5}$$

where Pr is the Prandtl number of the flow defined as,

$$Pr = \frac{v}{\alpha} \tag{6}$$

Eq. (5) is valid at low values of Pr, a typical case for molten metal flows. The resultant heat transfer relationship in terms of Nusselt number, $Nu = \frac{hx}{\kappa}$, can be related as [30],

$$Nu = \frac{1}{\sqrt{\pi}}(Re\ Pr)^{1/2} \tag{7}$$

However, in case the temperature of the plate is significantly lower than the temperature of the molten metal flowing on top, the result can be change in phase of the molten metal in the areas where the fluid particles have low flow velocities. At lower flow velocities the shearing stress is relatively large, i.e., in the viscous boundary layer region. In addition, the effect of temperature gradient is apparent in the thermal boundary layer region and, depending on the ratio $\frac{\delta_u}{\delta_T}$, the region within the viscous boundary layer is prone to phase change.

However, the thickness of viscous boundary layer varies especially at the entrance or start of the plate and gradually increases afterward to its maximum value. For the case of molten metal flows for casting purposes $Pr < 0.1$, suggests that the viscous boundary layer is quite small in thickness compared to thermal boundary layer. Therefore, the molten metal in the region of boundary layer thickness experiences thermal gradient at lower velocities and is highly likely to attain freeze (solid state). Therefore, the estimation of re-solidification of flowing molten metal can be related to the viscous boundary layer estimates.

In essence the problem of estimating freeze height, solidification height, is dependent on the heat balance at the interface. Considering the scenario presented in Fig. 1, the heat transfer is from the molten metal through convection and the solidified layer through conduction.

However, the solidification process involves an insensible heat transfer as well, latent heat of solidification. Thus at the steady state, the heat balance can be deduced as,

$$q_{latent} + Q_{convection} = Q_{conduction} \tag{8}$$

Or

$$\dot{m}\Delta H = \kappa A_s \frac{dT}{dy} - hA_s(T_m - T_s) \tag{9}$$

where $\dot{m}$ is the rate at which the mass of the molten metal freezes or solidifies and ΔH is the enthalpy difference amounting to the latent heat of solidification. While κ is the thermal conductivity of the solidified layer of metal, A_s is the surface area in contact, and h is the coefficient of convective heat transfer determined using Eq. (7). T_m and T_s are temperatures of the molten metal and the surface of the conduit respectively.

The contact area A_s can be calculated using,

$$A_s = H^a * L \tag{10}$$

where H^a is the resultant height of the channel through which molten metal passes while L is the width of the channel. Also note that the height of channel decreases with the formation of solidified metal layer at the bottom. Thus H^a can be calculated as,

$$H^a = H - dy \tag{11}$$

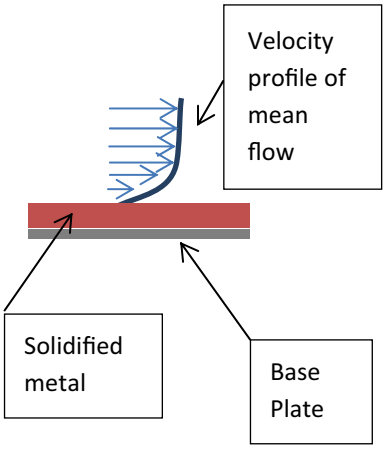

Figure 1 Schematics of the molten flow over a flat plate.

where H is the actual height of the channel and dy is the height of the solidified metal layer. Solution of Eq. (9) yields the height of freeze/solidification, varying along the channel.

However estimation of T_s is required for the exact calculation. The surface temperature depends on the heat balance of the channel with the surrounding cooling media. Neglecting the wall thickness of channel, heat balance between the solidified layer of metal and surrounding convection can be written as,

$$\kappa \frac{(T_s - T_\infty)}{x} = h_\infty (T_s - T_\infty) \tag{12}$$

where h_∞ is the convective heat transfer coefficient of the surrounding air with temperature T_∞. Thus using the effective wall temperature, the estimation of freeze height can be estimated at varying slope angles (θ) of the channel.

Fig. 2 presents the freeze height along the length of channel for various angles of the slope of the channel. It can be observed that thickness of the freeze decreases rapidly with the angle of inclination. This is primarily due to the increase in flow velocity of the molten metal with higher angle of inclination.

3. Experiment

In this study, commercial Al–Si aluminum alloy ASTM A356 is used. The composition of the ASTM A356 alloy is given in Table 1. The purpose of using sloping plate was efficient heat extraction and feedstock preparation. It also enabled us to control the process temperature. Molten metal about 800 °C is poured on sloping plate as shown in Fig. 3. Thermocouple was used to control the molten temperature. After preparing feedstock, slurry is poured into the mild steel die. Sloping channel of 800 mm length is prepared with stainless steel. Specimens are cast at 15°, 30°, 45°, 60° and 75° sloping plate angle. ASTM E8M Standard is for preparation of die used to cast tensile test specimen (Fig. 4 and Table 2) and the die used for the purpose is shown in Fig. 5.

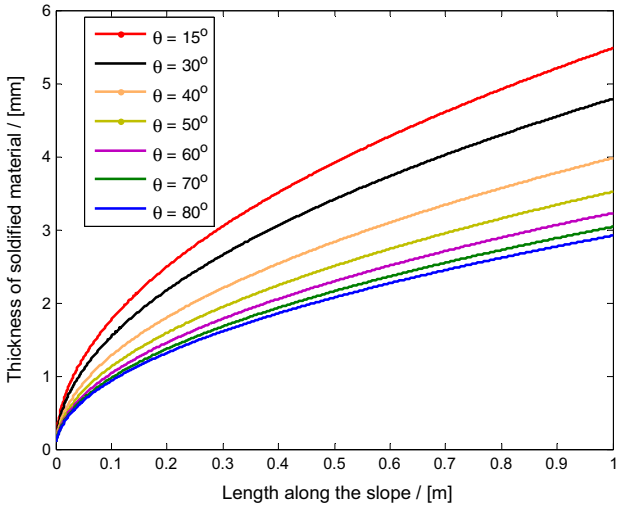

Figure 2 Prediction of thickness of solidified layer of molten metal along the slope of the channel at various angles of inclination.

Table 1 ASTM A356 chemical composition (ASTM B 26 – B 26 M – 03) wt%.

Aluminum	Silicon	Iron	Copper	Manganese	Magnesium	Zinc	Titanium
	6.5–7.5	0.6	0.25	0.35	0.20–0.45	0.35	0.25

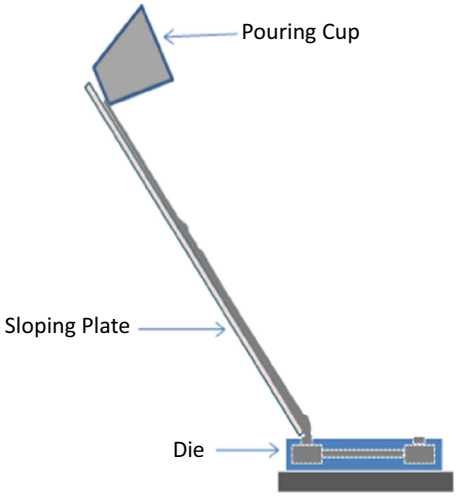

Figure 3 Experimental setup.

After that metallography on metallurgical microscope and hardness (Universal Hardness tester) and tensile testing on MTS 810 are done. Each experiment is repeated three (03) times.

4. Results

4.1. Effect of sloping plate angle variation on microstructure

In Fig. 6(a) 15° cast specimen shows elongated dendritic growth. Grain boundaries are visible and form tree like structure. Casting defect pores are also presented and seem equally dispersed. Precipitate morphologies are connected at grain boundaries and some independent crystals are visible. The connected precipitates cause high hardness and low toughness that is witnessed in hardness and elongation results, which will be discussed later. In Fig. 6(b) 30° cast sample also dendritic structure formed, irregular shape, deposition of eutectic phase is visible. Overall less porosity is observed but voids are formed which have elongated irregular shapes. Thicker precipitate morphology at grain is observed with boundaries but still having relatively continuous structures.

Table 2 ASTM E8M specimen specification.

G	Gage length	45
W	Width	12.5
T	Thickness	Thickness
R	Radius of fillet	12.5
A	Length of reduced section	60
B	Length of grip section	75
C	Width of grip section App.	20

In Fig. 6(c) 45° still dendritic growth occured with less porosity is formed. Grain structure is irregular and precipitate morphologies are thinner but still continuous. In Fig. 6(d) 60° grain of globular morphologies is formed. Some pores are also present. Precipitate is discontinuous but some cluster of precipitate is also visible. The matrix is more or less continuous. This specific microstructure allows for lower hardness and higher elongation. The values of Ultimate Tensile Strength are also improved above other angles. Apparently the grain refinement increases the sites for precipitate nucleation and promotes clustering of the precipitates, even though the actual grain size does not seem to be appreciably reduced. In Fig. 6 (e) 75° dendritic growth occured. Cracks are present and precipitate are thick and discontinuous.

At an inclination angle of 15°, 30°, and 45° the grain size is almost the same (see Fig. 7). At the highest sloping plate angle, 75° the grain size is decreased from 221 μm to 209 μm for a pouring temperature of 800 °C. The minimum grain size of 201 μm was obtained at 75° sloping angle and 800 °C.

4.2. Effect of sloping plate angle variation on ultimate tensile strength

Low flow velocities cause segregation of melt which produce non-uniform properties, and high velocities result in folding effect which results in shrinkages and voids. From the Fig. 8 it can be observed that Ultimate tensile strength (UTS) decreases up to sloping angle of 45°. From 45° up to 60°,

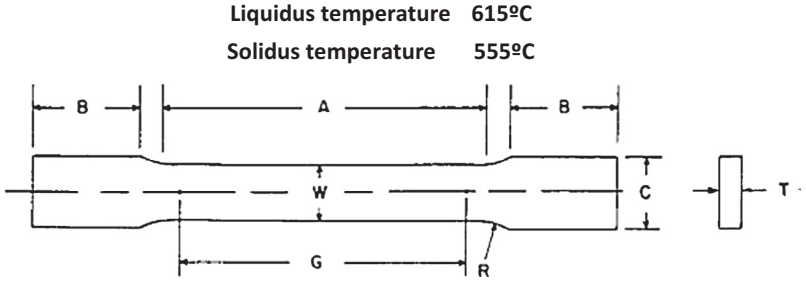

Figure 4 Cast specimen.

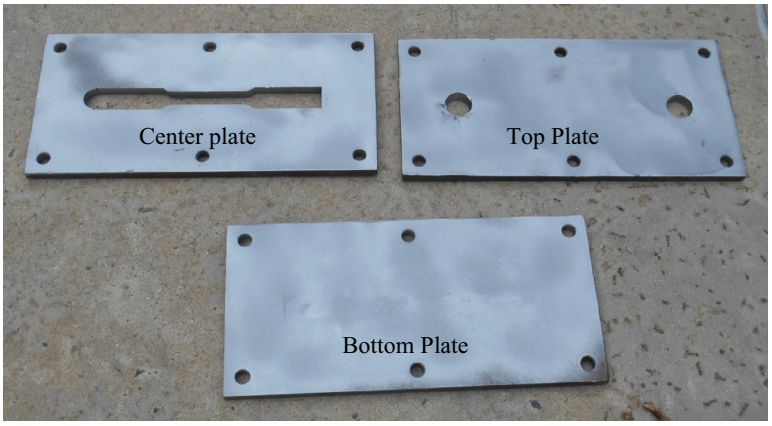

Figure 5 Un-assembled view of mild steel Die.

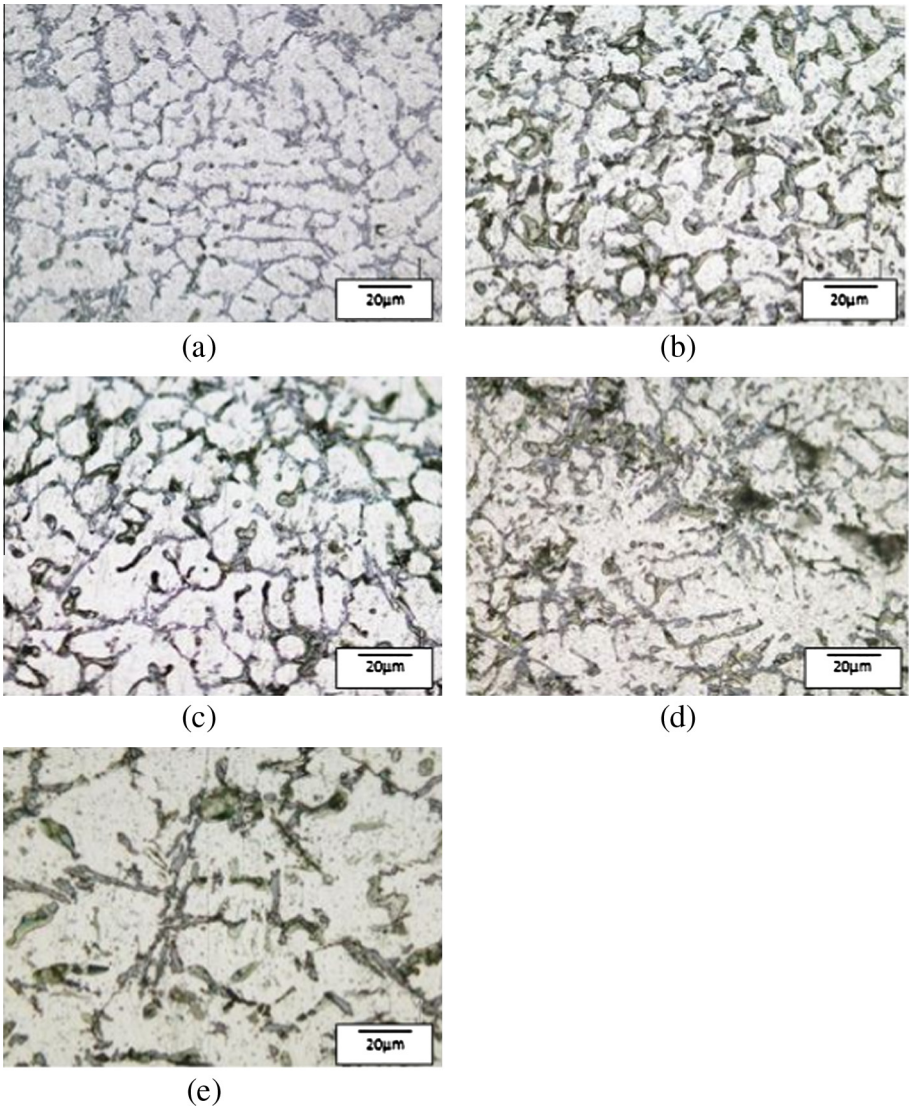

Figure 6 Different sloping angle cast specimen microstructure, scale: 20 μm 500× magnification. (a) Slope angle 15°, (b) slope angle 30°, (c) slope angle 45°, (d) slope angle 60°, and (e) slope angle 75°.

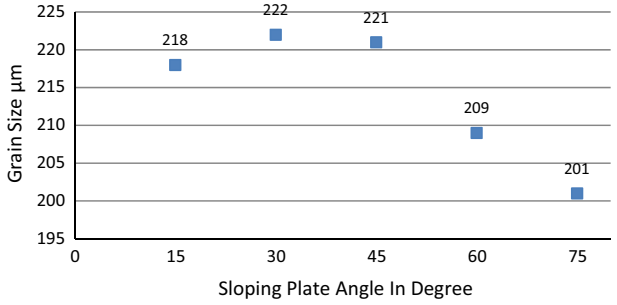

Figure 7 Sloping plate angle vs grain size.

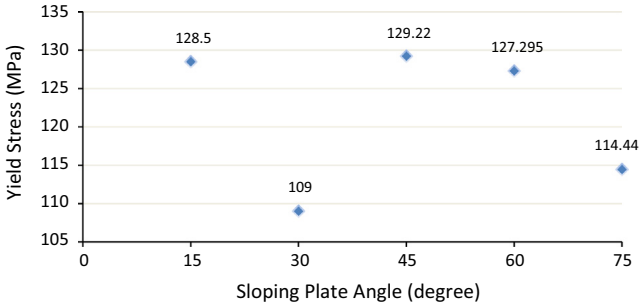

Figure 9 Sloping plate angle vs Yield Stress.

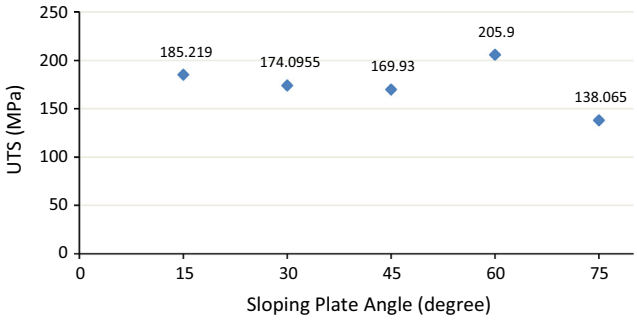

Figure 8 Sloping plate angle vs ultimate tensile strength.

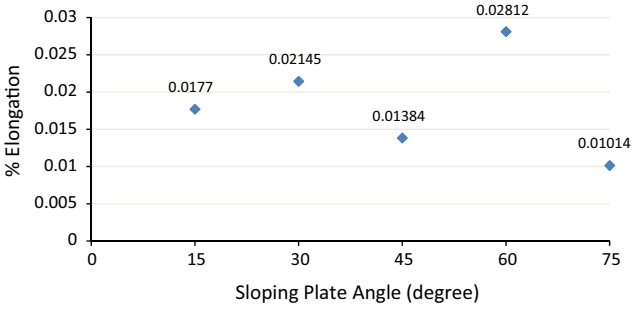

Figure 10 Sloping plate angle vs % elongation.

increasing trend of UTS is observed. The optimum angle for ASTM A356 Aluminum Alloy is 60°. At 75° again the value of ultimate tensile strength is at minimum level. It is seen that at very high angles (> 60°), a high amount of churning is seen as discussed earlier. This churning produces bi-layers within the solidified part. This bi-layer may be the principal cause of reduction in strength. A 33% loss of UTS is seen when sloping angle changes from 60° to 75°. On the other hand, at 60° at least 11% increase in the UTS is seen as compared to 15° sloping plate.

4.3. Effect of sloping plate angle variation on yield stress

From Fig. 9 it can be see that on 15°, 45° and 60° the value of yield stress is almost the same but at 30° anomalous behaviors are recorded with 14% lower value. Similar loss of yield stress is also observed in the 75° sloping plate sample.

4.4. Effect of sloping plate angle variation on percentage elongation

The alloy ASTM A356, in the as cast condition exhibits brittle behavior manifested as low elongation to rupture as seen in Fig. 10. After tensile testing 15° cast specimen experiences 1.7% elongation. Then elongation value is slightly increased up to 30° where 2.1% is recorded. % elongation follows a decreasing trend up to 45°, after that rate of elongation starts to increase and at 60° angle maximum percentage elongation of 2.8% is noted. Specimen cast at 60° angles has more ductility as compared to other cast angles. At region between 60° and 75°, it again decreases. It is expected that the churning effect and bilayer entrapment considerably reduce the elongation to rupture.

4.5. Effect of sloping plate angle variation on hardness

Brinell Hardness Number (BHN) at 15° is significantly high as compared to other angles as seen in Fig. 11. This high value corresponds well with the trend of low elongation of 15° samples. At 45°, 60°, and 75° only a slight variation is recorded. At 30° minimum value of BHN is recorded.

4.6. Effect of sloping plate angle variation on boundary layer thickness

At 30° and 45°, along the length of the plate thickness, deposited material boundary layer thickness is less as compared to 60° sloping channel. At 60° maximum heat transfer takes place and fraction of solid deposited on slope at this angle is maximum as shown in Fig. 12. The boundary layer thickness is expected to decrease with increasing angle as seen in Fig. 13. However, this is the case for 15° to 45° sloping angle. At 60° the boundary layer thickness increases dramatically. It is known that the heat transfer rate is strongly dependent on the flow velocity. Initially the increase in angle increases the velocity with the flow expectedly remains in the laminar regime and the boundary layer is not disturbed. The heat transfer rate in such a case is not expected to change appreciably. The higher velocity of the flowing fluid leads to decrease in boundary layer thickness and manifested as thinning of residual metal layer with increase in angle. However with further increase in flow velocity the assumption of laminar flow may no longer remains valid. Thus at 60° sloping plate angle, the

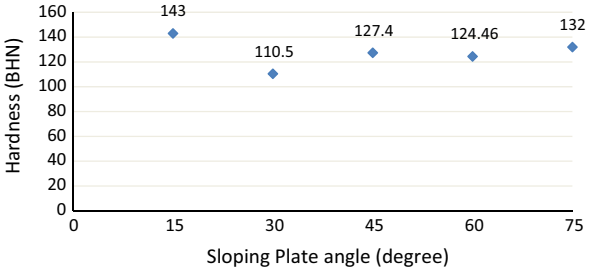

Figure 11 Sloping plate angle vs hardness.

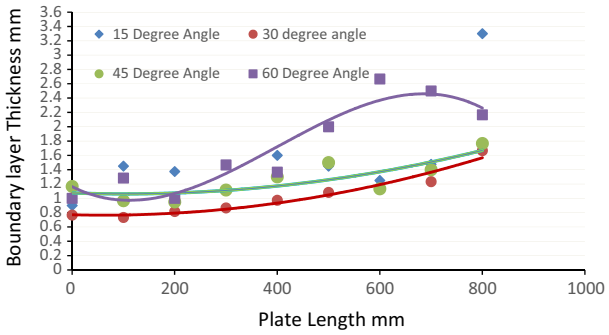

Figure 12 Sloping plate length vs boundary layer thickness.

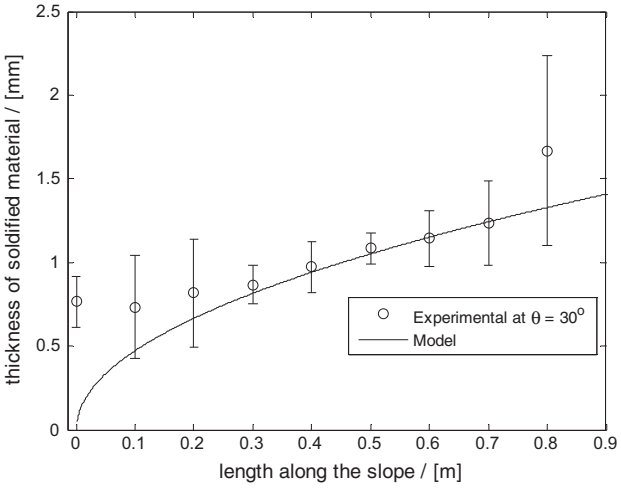

Figure 13 Comparison of thickness of boundary layer with the actual measurement of solidified layer of molten metal along the slope of the channel at 30° angle of inclination.

flow velocity apparently disrupts the boundary layer, and the turbulence causes a dramatic increase in heat transfer with decrease in boundary layer thickness. This increase in heat transfer causes a thicker solidified layer, giving rise to a thicker residual metal layer. The higher nucleation due to faster cooling will cause grain refinement effect. The overall increase in tensile properties also indicates this phenomenon. At higher velocities and slope angles, the effect of turbulence seems detrimental in calculating the effective heat transfer and nucleation rates, therefore requiring detailed investigation and CFD simulation. However modeling turbulence and its resultant effects are beyond the scope of this work.

The 75° slope angle causes severe churning and the residual metal layer is higly deformed. It thus gives no indication of the boundary layer formed and therefore not shown in Fig. 12.

4.7. Comparison of thickness of boundary layer with the simulated boundary layer

Using Eqs. (9) and (12), solution for the freeze height d_y is calculated for the values of variables provided in Table 1. For the case of Aluminum molten metal flow in a 30° slanted channel, the height of the solidified metal on the channel surface is compared with the experimental results. Fig. 13 shows the comparison of predicted freeze height and the measured heights. Experimental results are based on the average of three experimental runs at fixed slope angle. It is evident from Fig. that the predictions for the freeze height match with the experimental setup especially 0.2 m down the slope. A discrepancy between the predictions and the measured values can be observed at the entrance. This can be related to the entrance effects at the start of the slope as the liquid molten metal is poured in. Afterward a quite reasonable match can be seen.

5. Conclusion

Sloping plate grain refinement technique is used for the casting of ASTM A356 Al–Si alloy. Five slope plate angles of 15°, 30°, 45°, 60° and 75° are used for casting. Tensile and hardness tests reveal that sloping plate at the angle of 60° gives the highest tensile strength and elongation. The microstructure analysis reveals that clustering of the precipitates can be observed in a continuous matrix at 60° which gives the alloy highest tensile properties. At lower angles, precipitates are continuous with discontinuous matrix, giving this alloy a lower strength.

In order to investigate the influence of sloping angle, residual layer of solidified metal on the sloping plate is measured. The thicknesses are compared with the calculated boundary layer thicknesses using the analytical solution of the process. Observations suggest a sharp increase in the boundary layer thickness at slope angle of 60° which expectedly led to apparent improvements in the physical properties. Based on the analysis carried out here, it can be concluded that the sloping plate at 60° angle results in higher heat transfer rate in the melt, and therefore leads to increase in nucleation and grain refinement as well as causing minimum churning and bilayer effects.

References

[1] D. Spencer, R. Mehrabian, M.C. Flemings, Rheological behavior of Sn-15 pct Pb in the crystallization range, Metall. Trans. 3 (7) (1972) 1925–1932.
[2] D.H. Kirkwood, Semisolid metal processing, Int. Mater. Rev. 39 (1994) 173.
[3] Z. Fan, Semisolid metal processing, Int. Mater. Rev. 47 (2) (2002) 49–85.
[4] D.H. Kirkwood et al, Semi-solid processing of alloys, Springer Series in Materials Science, Vol. 124, 2010.
[5] K. Muszka, J. Majta, Ł. Bienias, Effect of grain refinement on mechanical properties of microalloyed steels, Metall. Foundry Eng. 32 (2006) 87–97.

[6] Y. Lee, A. Dahle, D. StJohn, The role of solute in grain refinement of magnesium, Metall. Mater. Trans. A 31 (11) (2000) 2895–2906.
[7] K. Kashyap, T. Chandrashekar, Effects and mechanisms of grain refinement in aluminium alloys, Bull. Mater. Sci. 24 (4) (2001) 345–353.
[8] R. Guan et al, Dynamical solidification behaviors and microstructural evolution during vibrating wavelike sloping plate process, J. Mater. Process. Technol. 209 (5) (2009) 2592–2601.
[9] X. Liu et al, Microstructure and mechanical properties of AZ91 alloy produced with ultrasonic vibration, Mater. Sci. Eng. A 487 (1) (2008) 120–123.
[10] X.-C. Qi et al, Influences of melt treatment on grain sizes and morphologies of AZ9 1D alloy, Trans. Nonferr. Met. Soc. China 17 (5) (2007) 887–892.
[11] D. Apelian, Aluminum Cast Alloys: Enabling Tools for Improved Performance, 2009.
[12] W. Winterbottom, Semi-solid forming applications: high volume automotive products, Metall. Sci. Technol. 18 (2) (2013).
[13] M. Kamran, Semi-solid processing of Al–Si7–Mg alloys (PhD thesis), Metallurgy Department, University of Leoben, 2008.
[14] T. Haga et al, Twin roll casting of aluminum alloy strips, J. Mater. Process. Technol. 153 (2004) 42–47.
[15] R. Guan et al, Heat transfer and grain refining mechanism during melt treatment by cooling sloping plate, Acta Metall. Sin. (Engl. Lett.) 25 (4) (2012) 320–328.
[16] X. Wang et al, Boundary layer distributions and cooling rate of cooling sloping plate process, J. Wuhan Univ. Technol.-Mater. Sci. Ed. 28 (4) (2013) 701–705.
[17] Z.Y. Huang, Mathematic model of solid fraction during rheo-casting by the cooling sloping plate process, Acta Metall. Sin. (Engl. Lett.) 25 (1) (2012) 81–88.
[18] T. Haga, S. Suzuki, Casting of aluminum alloy ingots for thixoforming using a cooling slope, J. Mater. Process. Technol. 118 (1) (2001) 169–172.
[19] H. Watari et al, Semi-solid manufacturing process of magnesium alloys by twin-roll casting, J. Mater. Process. Technol. 155 (2004) 1662–1667.
[20] A. Muumbo, M. Takita, H. Nomura, Processing of semi-solid gray cast iron using the cooling plate technique, Mater. Trans. 44 (5) (2003) 893–900.
[21] N. Poolthong, H. Nomura, M. Takita, Effect of heat treatment on microstructure, wear properties and corrosion characteristics of semi-solid processed high chromium cast iron, Int. J. Cast Met. Res. 16 (6) (2003) 573–578.
[22] R. Ritwik, A.P. Rao, B. Dhindaw, Low-convection-cooling slope cast AlSi7Mg alloy: a rheological perspective, J. Mater. Eng. Perform. 22 (9) (2013) 2487–2492.
[23] R. Guan et al, Three-dimensional analysis of the modified sloping cooling/shearing process, J. Univ. Sci. Technol. Beijing, Mineral Metall. Mater. 14 (2) (2007) 146–150.
[24] R.-G. Guan et al, Novel sloping plate process for semisolid metal forming, Mater. Sci. Technol. 23 (4) (2007) 438–443.
[25] Y.M.a.Y. Hao, Grain refinement of AZ31 alloy via self-inoculation, Adv. Mater. Res. 1030–1032 (2014) 108–111.
[26] D. Brabazon, D. Browne, A. Carr, Mechanical stir casting of aluminium alloys from the mushy state: process, microstructure and mechanical properties, Mater. Sci. Eng. A 326 (2) (2002) 370–381.
[27] M. Jaworski et al, Thermoelectric magnetohydrodynamic stirring of liquid metals, Phys. Rev. Lett. 104 (9) (2010) 094503.
[28] R. Haghayeghi et al, An investigation on DC casting of a wrought aluminium alloy at below liquidus temperature by using melt conditioner, J. Alloy. Compd. 502 (2) (2010) 382–386.
[29] D.J. Tritton, Physical Fluid Dynamics, Van Norstrand Reinhold, Berkshire, England, 1980.
[30] W.A. Khan, J.R. Culham, M.M. Yovanovich, Analytical study of heat transfer from circular cylinder in liquid metals, J. Heat Mass Transfer 42 (11) (2006) 1017–1023, Springer-Verlag.